GDF15 mediates renal cell plasticity in response to potassium depletion in mice

Samia Lasaad, Christine Walter, Chloé Rafael, Luciana Morla, Alain Doucet, Nicolas Picard, Anne Blanchard, Yves Fromes, Béatrice Matot, Gilles Crambert, et al.

Received: 31 March 2023 | Revised: 17 August 2023 | Accepted: 23 August 2023

DOI: 10.1111/apha.14046

ACTA PHYSIOLOGICA

RESEARCH PAPER

GDF15 mediates renal cell plasticity in response to potassium depletion in mice

Samia Lasaad[1,2] | **Christine Walter**[1,2] | **Chloé Rafael**[1,2] | **Luciana Morla**[1,2] | **Alain Doucet**[1,2] | **Nicolas Picard**[3] | **Anne Blanchard**[1,2,4] | **Yves Fromes**[5] | **Béatrice Matot**[5] | **Gilles Crambert**[1,2] | **Lydie Cheval**[1,2]

[1]Laboratoire de Physiologie Rénale et Tubulopathies, Centre de Recherche des Cordeliers, INSERM, Sorbonne Université, Université Paris Cité, Paris, France

[2]CNRS EMR 8228 – Unité Métabolisme et Physiologie Rénale, Paris, France

[3]Laboratory of Tissue Biology and Therapeutic Engineering, UMR 5305 CNRS, University Lyon 1, Lyon, France

[4]Assistance Publique Hôpitaux de Paris, Hôpital Européen Georges Pompidou, Centre d'Investigation Clinique, Paris, France

[5]NMR Laboratory, Neuromuscular Investigation Center, Institute of Myology, Paris, France

Correspondence
Gilles Crambert, Laboratoire de Physiologie Rénale et Tubulopathies, Centre de Recherche des Cordeliers, 15 rue de l'Ecole de Médecine, 75270 Paris Cedex, France.
Email: gilles.crambert@crc.jussieu.fr

Funding information
Agence Nationale de la Recherche; Ministère de l'Enseignement Supérieur et de la Recherche Scientifique

Abstract

Objective: To understand the mechanisms involved in the response to a low-K^+ diet (LK), we investigated the role of the growth factor GDF15 and the ion pump H,K-ATPase type 2 (HKA2) in this process.

Methods: Male mice of different genotypes (WT, GDF15-KO, and HKA2-KO) were fed an LK diet for different periods of time. We analyzed GDF15 levels, metabolic and physiological parameters, and the cellular composition of collecting ducts.

Results: Mice fed an LK diet showed a 2–4-fold increase in plasma and urine GDF15 levels. Compared to WT mice, GDF15-KO mice rapidly developed hypokalemia due to impaired renal adaptation. This is related to their 1/ inability to increase the number of type A intercalated cells (AIC) and 2/ absence of upregulation of H,K-ATPase type 2 (HKA2), the two processes responsible for K^+ retention. Interestingly, we showed that the GDF15-mediated proliferative effect on AIC was dependent on the ErbB2 receptor and required the presence of HKA2. Finally, renal leakage of K^+ induced a reduction in muscle mass in GDF15-KO mice fed LK diet.

Conclusions: In this study, we showed that GDF15 and HKA2 are linked and play a central role in the response to K^+ restriction by orchestrating the modification of the cellular composition of the collecting duct.

KEYWORDS

ATP12A, cell proliferation, ErbB2, muscle potassium storage, potassium homeostasis

1 | INTRODUCTION

The modern Western diet is characterized by consumption of processed food and high intakes of protein, high-fat dairy products, and high-sugar drinks, correlating with development of metabolic disorders (diabetes, obesity). This diet also has profound but often underappreciated impacts on electrolyte balance. Indeed, a human consuming the typical Western diet produces approximately 50 mmol of acid/day whereas our ancestors were

considered to be net base producers.[1] In parallel, the consumption of salt (NaCl) and potassium (K^+) has been completely changed, shifting from a rich K^+/low NaCl diet in hunter-gatherer populations to the opposite (low-K^+/rich NaCl diet) in the modern, westernized population.[2] In a recent study, we showed that the median daily Na^+ and K^+ intakes of young Parisian males are 136 and 57 mmol/day, respectively,[3] which are far from the recommended dietary reference intakes (maximal Na^+ intake 65 mmol/day and minimal K^+ intake 120 mmol/day). Fortunately, our kidneys have allowed us to cope with these relative recent changes in our eating habits. However, in the long-term, these dietary modifications may contribute to the development of diseases such as hypertension[4] and are correlated with a higher risk of mortality[5] when they encounter favorable genetic backgrounds with polymorphisms that would have otherwise remained silent under a more "natural" diet. It is well known that the lack of K^+ in the diet can induce a global adaptation involving coordinated regulatory processes.[6] The ability of muscle to release K^+ (internal balance) is of particular importance for rapidly modulating the plasma K^+ concentration.[7] Concurrently, the kidney decreases K^+ secretion (through inhibition of K^+ channel ROMK, for review see Ref. 8) and activates K^+ retention pathways through both progesterone-dependent stimulation of H,K-ATPase type 2[9] and increasing number of A-type intercalated cells (AIC) in the collecting duct.

The cellular plasticity of the collecting duct is a fascinating ability that allows the kidney to modify its structure to respond to ionic stress through mechanisms involving either transdifferentiation between different cell types within collecting ducts[10] or direct cell proliferation.[11] Our group has identified that the growth differentiation factor 15 (GDF15) triggers the proliferation of AIC in response to acidosis.[12,13] GDF15 is a peptide belonging to the TGFβ family, which has been reported to have multiple physiological effects.[14] In addition to its production in the collecting duct, it has also been established that GDF15 is produced by a subset of proximal tubule cells in mice mimicking Cockayne syndrome.[15] It is now strongly suggested that GDF15 is a sentinel mediator[16] that responds to stress involving mitochondrial defects[17–19] and is found in increased concentration in blood and urine following many pathological states, most prominently, cancer. GDF15 also helps control energy metabolism, as it has been found to be overexpressed during obesity[20,21] and has anorectic properties.[22,23] GDF15 may also help protect against inflammation, tissue injury, and muscle wasting as it has been shown that GDF15 increases with aging.[24] Interestingly, GDF15 has also been identified as one of the most upregulated genes in mouse kidney collecting ducts in response to a total dietary K^+-restriction,[11] which is a stronger stress than that occurring in western diet, but its role in this particular situation was yet unknown.

2 | RESULTS

2.1 | GDF15 level is increased in response to dietary K^+-restriction

We showed that urine GDF15 is increased (Figure 1A) by K^+ restriction following a time course that ends to a plateau at day 3–4. At this plateau, the level of GDF15, normalized to the creatinine, is 3-time higher than in control diet (877 ± 104 ng/mmol at day 4 vs. 310 ± 25 ng/mmol in control diet). In parallel, the level of GDF15 in the plasma (Figure 1B) is also 2-time higher in mice under low-K^+ diet for 4 days than under control diet (140 ± 14 vs. 69 ± 2 pg/mL, respectively). As shown in Figure 1C, the expression of GDF15 is increased to a different extent in all tubular segments from mice under low-K^+ diet. Since the stimulation of GDF15 is more systemic than previously envisaged, we therefore extended our investigation to muscle tissues and intestine, which are known to be involved in K^+ metabolism. As shown in Figure 1D, we measured the tissue content of GDF15 by ELISA analysis we showed that it is significantly increased in the ileum and the colon but not in muscle of mice under K^+ restriction.

2.2 | GDF15 participates in the renal adaptation to K^+-restriction through an ErbB2-dependent mechanism

The physiological parameters of WT and GDF15-KO mice were reported in Table 1. After 14 days of LK diet, the weight of WT mice is lower than that of GDF15-KO mice. Urine volume increased in both genotypes. Measurement of the urine K^+ excretion of WT and GDF15-KO mice in response to an LK diet (Figure 2A) showed that the absence of GDF15 induced a delayed in the reduction of K^+-excretion. Thus, at days 1, 2, and 3 of the K^+-restriction period, the daily K^+ excretion was increased up to 100% in GDF15-KO mice compared to WT mice. As shown in Figure 2B, this delayed renal response has a consequence on the plasma K^+ level at Day 4 of the LK diet, with GDF15-KO mice becoming hypokalemic (3.3 ± 0.1 mM) compared with their value under normal K^+ diet (4.3 ± 0.2 mM, $p < 0.01$). On the contrary, WT mice remained with a normal plasma K^+ value (3.9 ± 0.1 mM) after 4 days of LK diet, which is not different from that measured in normal K^+ diet (4.1 ± 0.1 mM). Therefore, after 4 days of

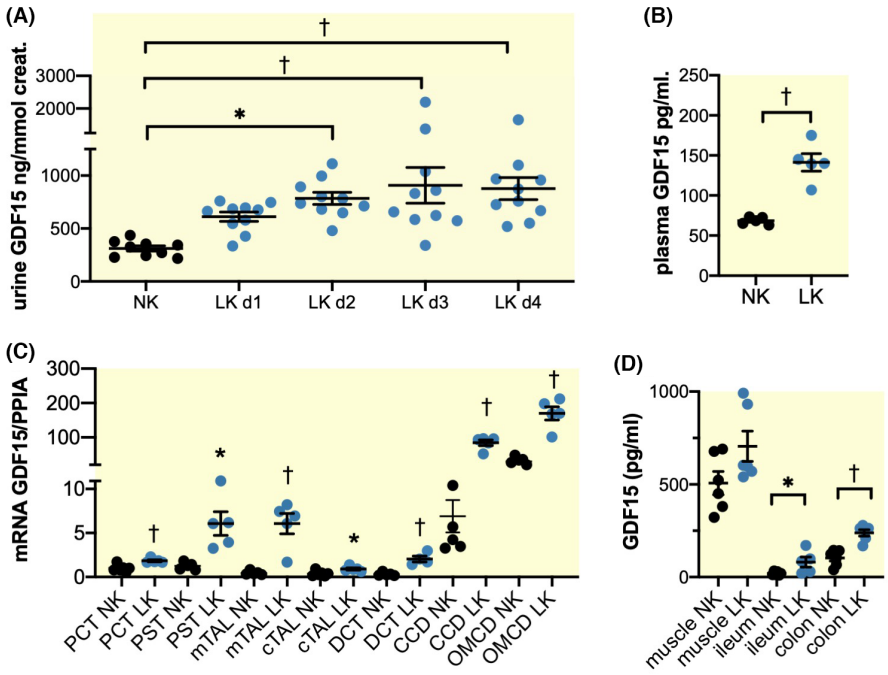

FIGURE 1 GDF15 is produced in response to K^+ restriction. (A) Urine GDF15 normalized by urine creatinine under control condition (NK, empty symbols) and at Days 1–4 of a low-K^+ diet period (LK, filled symbols). Results are shown as mean ± s.e.m (two series, $n = 10$) and analyzed by a one-way ANOVA test ($p < 0.01$) followed by a Dunett's multiple comparison test with NK group as a control group ($^{\dagger}p < 0.01$; $^{*}p < 0.05$). (B) Plasma GDF15 level in mice under normal diet (NK, empty symbols) or K^+-restriction for 4 days (LK, filled symbols). Results are shown as mean ± s.e.m (one series, $n = 4$–5) and analyzed by an unpaired Student t test ($_{\dagger}p < 0.01$). (C) mRNA expression of GDF15 in isolated proximal convoluted tubules (PCT), proximal straight tubules (PST), medullary and cortical thick ascending limb (m and cTAL), distal convoluted tubule (DCT) and cortical or outer medullary collecting duct (CCD and OMCD) of mice under normal diet (NK, empty symbols) or K^+-restriction for 4 days (LK, filled symbols). Results are shown as mean ± s.e.m (one series, $n = 5$) and analyzed by comparing the effect of the diet on each segment independently of the others by a Mann–Whitney test ($^{\dagger}p < 0.01$; $^{*}p < 0.05$). (D) GDF15 protein expression was measured in muscle (gastronecmius), ileum, and distal colon tissues by ELISA in mice under normal diet (NK, empty symbols) or K^+-restriction for 4 days (LK, filled symbols). Results are shown as mean ± s.e.m (one series, $n = 6$) and analyzed by a Mann–Whitney test ($^{\dagger}p < 0.01$).

TABLE 1 Physiological parameters of WT or GDF15-KO, under normal (NK) or low-K^+ diet (LK) from the same mice in metabolic cages as in Figure 2A.

	Day 1 NK		Day 4 LK		Day 14 LK	
Genotype	**WT**	**GDF15-KO**	**WT**	**GDF15-KO**	**WT**	**GDF15-KO**
Weight (g)	23 ± 1.3	26 ± 1	22 ± 1.4	26 ± 1	20 ± 1.2	26 ± 1**
Food intake (g)	4.2 ± 0.2	3.8 ± 0.3	2.7 ± 0.2	3.3 ± 0.3	2.7 ± 0.2	3.1 ± 0.2
Urine vol. (mL)	1.2 ± 0.2	1.7 ± 0.7	2.4 ± 0.4	3.6 ± 0.6	4.2 ± 0.6	5.7 ± 0.3

Note: Results are shown as mean ± s.e.m. Two-way ANOVA test followed by a Sidak's multiple comparisons test (WT vs. GDF15-KO mice at day 14 LK, $^{**}p < 0.01$), bodyweight is neither significantly impacted by the genotype of the mice nor the treatment (diet period) condition ($p < 0.01$) but by the interaction of both ($p < 0.01$).

LK diet, GDF15-KO mice exhibited a significantly lower plasma K^+ value compared with WT mice (3.3 ± 0.1 mM vs. 3.9 ± 0.1 mM). At Day 10, both genotypes exhibited a similar and decreased plasma K^+ value around 3.2 mM. These results indicate that the GDF15-KO mice are more sensitive to K^+ restriction than WT mice by developing hypokalemia more rapidly.

2.3 | GDF15 is involved in the increase of AIC observed in response to LK diet

To quantify the increase of AIC number, we used a simple method (fully described and validated in Ref. 25) consisting of isolation of medullary collecting ducts and labeling of anion exchanger 1 (AE1), a specific marker

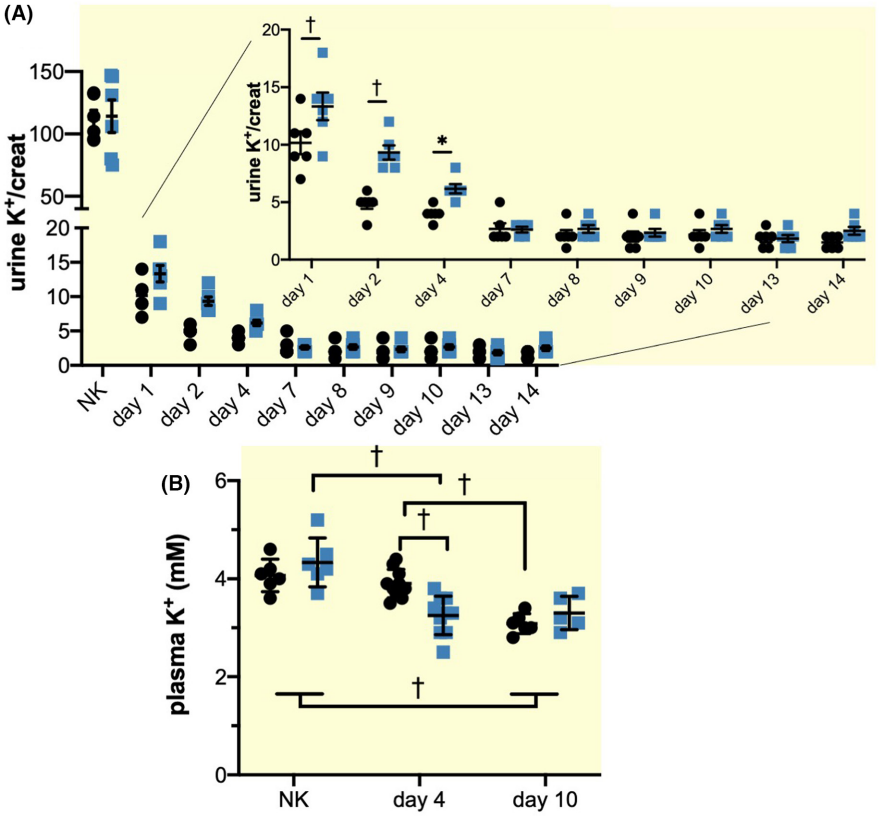

FIGURE 2 GDF15 regulates K^+ balance under low-K^+ diet. (A) Urine K^+ excretion normalized by urine creatinine under control condition (NK) and at Days 1–14 of a low-K^+ diet (LK) in WT (black circles) or GDF15-KO (blue squares) mice (same animals throughout the experiment). *Inset*: close-up of the LK period. Results are shown as mean ± s.e.m (one series, $n = 6$) and analyzed by a two-way ANOVA (factors: genotype and time under LK diet). followed by a Sidak's multiple comparison test on the LK period ($^{\dagger}p < 0.01$; $^{*}p < 0.05$). Urine K^+ excretion under LK diet is significantly impacted by the genotype of the mice ($p = 0.017$), by the time ($p < 0.01$), and by the interaction of both ($p < 0.01$). (B) On a different series of animals, we measured the plasma K^+ level under control condition (NK) and at Days 4 and 10 of a low-K^+ diet (LK) in WT (circles) or GDF15-KO (squares) mice. Results are shown as mean ± s.e.m (one series, $n = 6$–8) and analyzed by a two-way ANOVA followed by a Sidak's multiple comparison test ($^{\dagger}p < 0.01$; $^{*}p < 0.05$). Plasma K^+ level is not significantly impacted by the genotype of the mice but depends on the time of exposure to LK diet ($p < 0.01$) and the interaction of both ($p < 0.01$).

of AIC (Figure 3A). As shown in Figure 3B, the number of cells per mm is modified neither by the K^+-restriction period nor by the absence of GDF15 (GDF15-KO). However, the percentage of AE1+ cells in WT mice increased from 20.8 ± 0.7% in control diet to 23.7 ± 0.6% ($p < 0.05$) under K^+-restriction (Figure 3C). In GDF15-KO mice fed a control diet, the percentage of AIC is similar to that in WT mice and did not increase in the LK diet condition (20.9 ± 0.4% vs. 21.2 ± 0.8%, respectively). Because a defining characteristic of AIC is to be completely isolated in the tubular epithelium, the observation of two adjacent cells (a doublet) is therefore evidence of a recent cell division. As shown in Figure 3D, the number of AIC doublets was significantly increased by a low-K^+ diet in WT mice (13.8 ± 1.8 doublets/mm and 21.1 ± 1.4 doublets/mm, respectively, $p < 0.05$). In GDF15-KO mice, the number of doublets is similar to that of WT mice under control diet and did not increase after 4 days of LK diet. The expression of Cyclin D1, a gene involved in cell proliferation, was then analyzed in isolated OMCD of WT and GDF15-KO mice fed either control diet or 2 or 4 days of LK diet. As shown in Figure 3E, cyclin D1 expression in OMCD is similar in both mouse genotypes but is significantly increased after 2 days of LK diet in WT ($p < 0.01$) but not in GDF15-KO mice, indicating a delay in cell division rates in the absence of GDF15. After 4 days of LK diet, both genotypes expressed the same amount of cyclin D1 in their OMCD. Another hallmark of the renal response to K^+ restriction is an increase in expression of H,K-ATPase type 2. As shown in Figure 3F, the absence of GDF15 completely impeded stimulation of the catalytic subunit of HKA2 (ATP12A).

2.4 | The HKA2 is required for AIC proliferation

Cell division requires stimulated uptake of K^+ (through stimulation of Na,K-ATPase activity[26,27]) and an increased

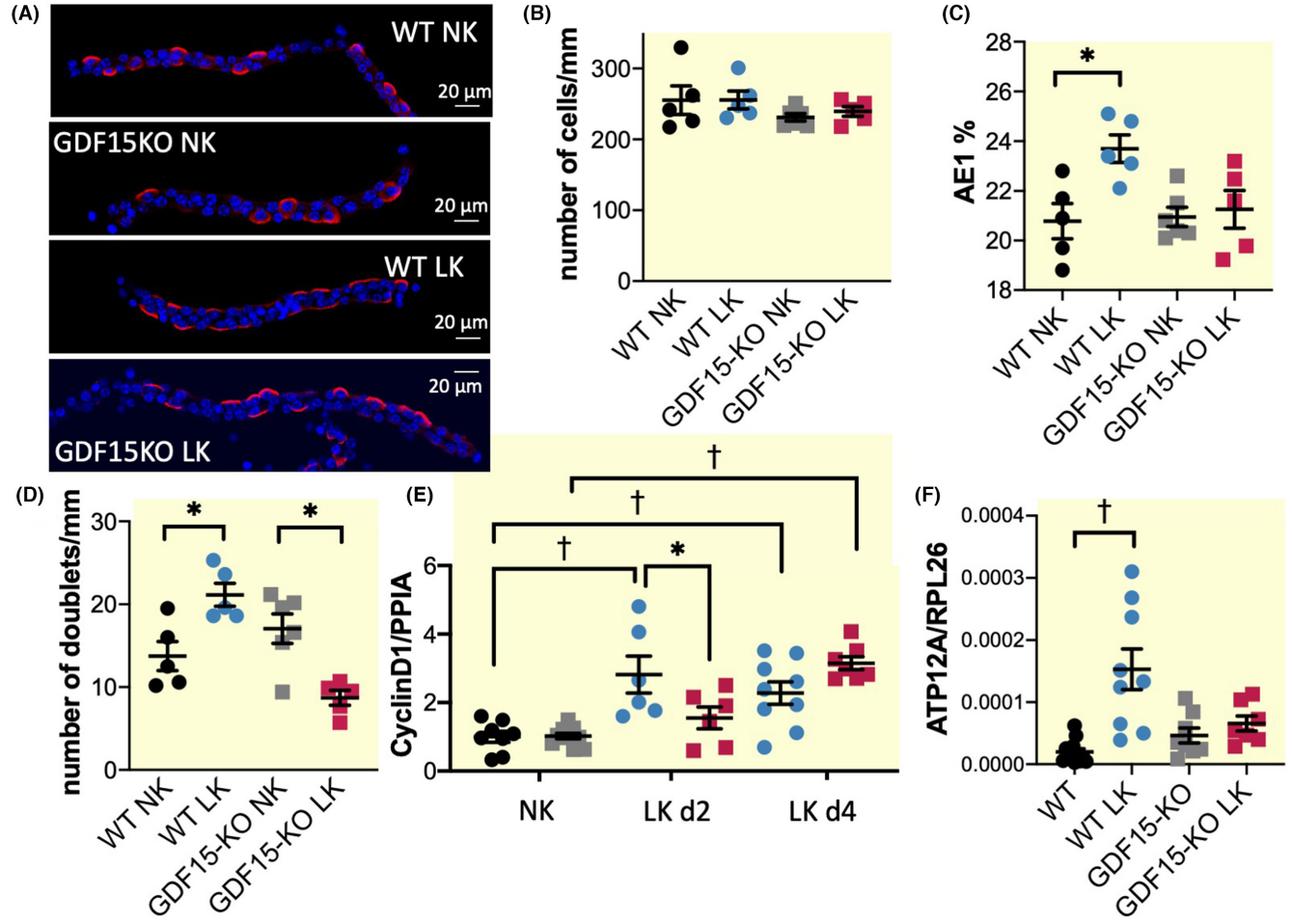

FIGURE 3 GDF15 is involved in proliferation of ICA under low-K^+ diet. (A) Examples of immunofluorescence pictures obtained by confocal microscopy from isolated OMCD from WT (blue circles) or GDF15-KO (red squares) mice under normal (empty symbols) or K^+-restriction for 4 days (filled symbols) labeled with DAPI (blue) and anti-AE1 antibody (red). The stacks of these images were then used to reconstruct tubules in 3D in order to accurately count the number of nucleus (B), the percentage of AE1+ cells (C) and the number of AE1+ doublet (at least two AE1 + cells with cell–cell contact, (D). Each symbol represents the mean value of 7–11 reconstructed tubules of the same animal. Results are shown as mean ± s.e.m (two series, $n = 5–6$) and analyzed by a Mann–Whitney test ($^{\dagger}p < 0.01$). (E) Cyclin D1 mRNA expression in OMCD of WT (circles) or GDF15-KO mice (squares) under normal (empty symbols) or K^+-restriction (filled symbols) for 2 and 4 days (one series, $n = 6–10$). Results are shown as mean ± s.e.m and analyzed by a two-way ANOVA followed by a Sidak's multiple comparison test. Cyclin D1 expression is strongly affected by the period of the K^+-restriction ($p < 0.01$) and by the combination of both treatment period and genotype ($p < 0.01$) but not by the genotype itself ($p = 0.25$). (F) ATP12A mRNA expression in OMCD of WT (circles) or GDF15-KO mice (squares) under normal (empty symbols) or K^+-restriction (filled symbols) for 4 days ($n = 6–10$). Results are shown as mean ± s.e.m. and analyzed by a one-way ANOVA test ($p < 0.01$) followed by a Tukey's multiple comparison test ($^{\dagger}p < 0.01$).

capacity for H^+ extrusion (through stimulation of Na,H-exchanger activity)[28] to avoid shrinkage and apoptosis (for review, see Ref. 29), two requirements that could also be met by the HKA2. We therefore investigated the parameters for cell proliferation in HKA2-KO mice under low-K^+ diet. First, we showed that HKA2-KO mice increased the expression of GDF15 in their collecting ducts in response to low-K^+ diet, as observed in WT mice (Figure 4A). HKA2-KO mice also showed an increase of PCNA and cyclinD1 expression, two markers of proliferation similar to that of WT mice (Figure 4B,C), indicating that the signal to proliferate has been received and integrated. However, the number of cells/mm, the percentage of AE1+ cells, and the number of doublets/mm remained unchanged in HKA2-KO mice indicating that AIC did not proliferate as expected (Figure 4D–F). To understand why, despite the increased expression of markers of proliferation, the number of cells remained unchanged in HKA2-KO mice, we measured apoptosis using TdT-mediated dUTP nick end-labeling (TUNEL). We observed that collecting ducts from low-K^+ diet fed HKA2-KO mice exhibited a 3–4 times higher number of TUNEL+ cells than those from low-K^+ diet fed WT mice in the same condition (Figure 5A). In AIC undergoing cell division, the absence of HKA2 may

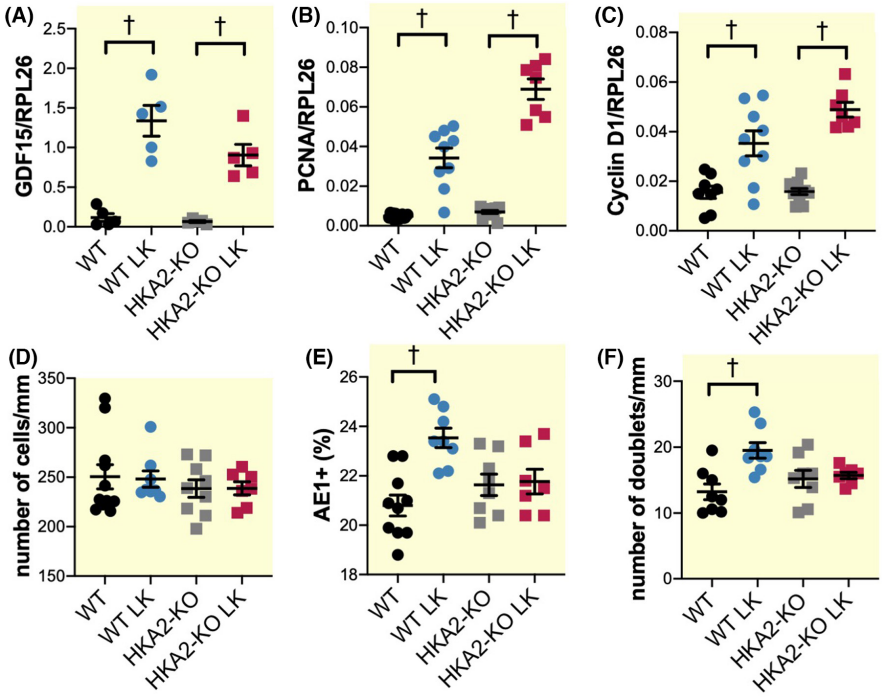

FIGURE 4 HKA2 is involved in proliferation of ICA under low-K^+ diet. (A–C) mRNA expression of GDF15, PCNA and CyclinD1 in isolated OMCD of WT (circles) or HKA2-KO mice (squares) under normal (empty symbols) or K^+-restriction (filled symbols) for 4 days. Results are shown as mean ± s.e.m (one series, $n = 5–9$) and a one-way ANOVA test ($p < 0.01$) followed by a Tukey's multiple comparison test ($^{\dagger}p < 0.01$). (D–F) The number of cells/mm, the percentage of AE1+ cells/mm and the number of AE1+ doublet/mm. Each symbol represents the mean value of 7–11 reconstructed tubules of the same animal. Results are shown as mean ± s.e.m (two series, $n = 5–6$) and analyzed by one-way ANOVA test and Tukey's post-test ($^{\dagger}p < 0.01$; $^{*}p < 0.05$).

result in cell shrinkage because K^+ uptake is not efficient enough to fill the intracellular volume and provide a high K^+ concentration and a drop in intracellular pH, two conditions that could trigger ER stress in a context where cell proliferation is triggered by GDF15. Moreover, an ER stress component such as CHOP is known to induce apoptosis upon strong stimulation. As shown in Figure 5B,C, CHOP expression is significantly stimulated in HKA2-KO mice under low-K^+ diet compared to normal dietary condition or to WT mice under low-K^+ diet.

2.5 | ErbB2 receptor mediates GDF15 renal effects

The classic receptor for GDF15 that mediates most of its central nervous effect and metabolic effects (for review, see Ref. 30) is GFRAL. This receptor is not present in the kidney[25] but we have recently identified that the ErbB2 receptor, another receptor of GDF15, was present in the kidney,[25] and mediates the GDF15 proliferative effect during acidosis. In Figure 6A, we measured ErbB2 expression in whole kidney and cortical (CCD) and the medullary collecting duct (OMCD). We observed that ErbB2 is not modified by an LK diet at the level of whole kidney analysis but is significantly increased in the distal nephron by 50%–100% in response to K^+-restriction. This indicates that ErbB2 may be involved in the GDF15-dependent renal response to K^+-restriction. We tested this hypothesis by treating WT mice under either control or LK diet for 4 days with an antagonist of ErbB2, mubritinib. As shown in Figure 6B, mubritinib treatment did not modify the number of cell/mm but impeded the LK diet-dependent increase in AIC (Figure 6C,D). Interestingly, the absence of AIC proliferation under a low-K^+ diet impedes correct adaptation. Mubritinib treatment alone did not impact the plasma K^+ level of mice under control diet; however, it reduced the plasma K^+ values of WT mice fed LK diet for 4 days (nontreated mice 4.0 ± 0.2 mM vs. treated mice 3.3 ± 0.1 mM, $p < 0.05$, Figure 6E). The regulation of cell plasticity in collecting ducts by a GDF15/ErbB2 axis could therefore be essential to renal adaptation to a dietary K^+ restriction.

2.6 | The absence of GDF15 induces modification of muscle structure in response to K^+ restriction

Since muscles participate in the K^+ balance by releasing their intracellular K^+ into the extracellular compartment,

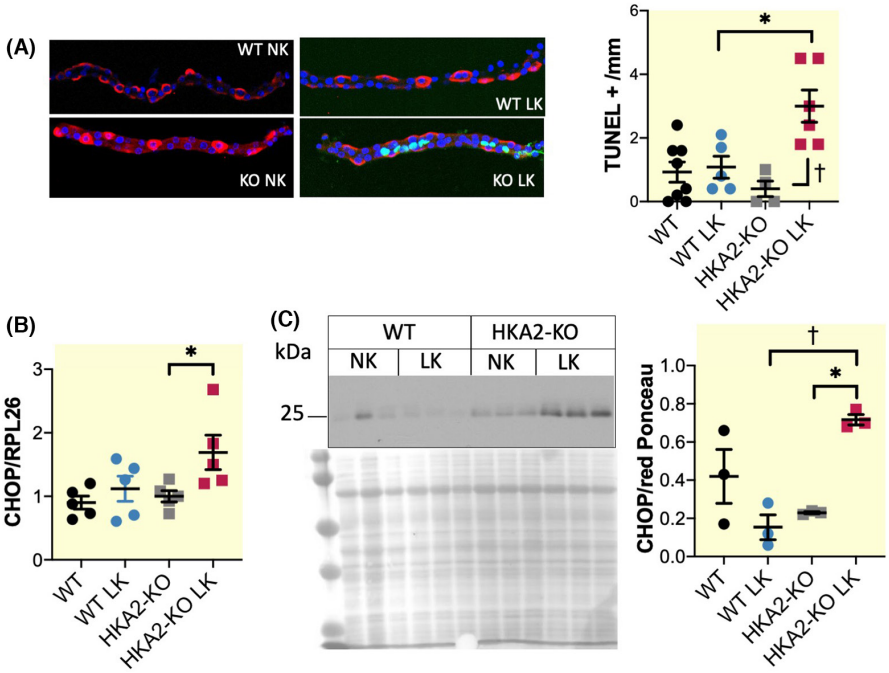

FIGURE 5 HKA2 protects against ER stress and apoptosis during proliferation under low-K^+ diet. (A) Examples of immunofluorescence pictures obtained by confocal microscopy from isolated OMCD after labeling for apoptotic cells (TUNEL, green), nucleus (DAPI, blue) and AIC (anti-AE1 antibody, red). The number of TUNEL+ cells were then counted and normalized by the length of the tubules. Results are shown as mean ± s.e.m (one series, $n = 5–6$) and analyzed by one way ANOVA test and Tukey's post-test ($^{\dagger}p < 0.01$; $^{*}p < 0.05$). (B) CHOP mRNA expression in WT (circles) or GDF15-KO mice (squares) under normal (empty symbols) or K^+-restriction (filled symbols) for 4 days (one series, $n = 5$). Results are shown as mean ± s.e.m. and analyzed by a one-way ANOVA test ($p < 0.01$) followed by a Tukey's multiple comparison test ($^{\dagger}p < 0.01$). (C) CHOP protein expression in total kidney lysate from WT (circles) or GDF15-KO mice (squares) under normal (empty symbols) or K^+-restriction (filled symbols) for 4 days (one series, $n = 3$).

we measured the muscle K^+ contents of the WT and GDF15-KO mice under normal or K^+ depleted conditions.

As shown in Figure 7A, under normal conditions, muscles (gastrocnemius) of WT mice contained 20% significantly more K^+ than those from GDF15-KO mice. This result suggests that the GDF15-KO mice already compensate for the lack of GDF15 by releasing muscle K^+. As expected, muscle K^+ content is significantly decreased in WT mice after 4 days of K^+ restriction compared to the control condition (66 ± 3 vs. 82 ± 2 μmol/g, respectively). Conversely, GDF15-KO mice, which have already a low muscle K^+ content under normal conditions, are unable to decrease it even more (68 ± 3 vs. 61 ± 5 μmol/g). We then investigated whether the muscle structure was modified in response to K^+ restriction and found that, in this condition, WT muscles have larger fibers than GDF15-KO mice (2148 ± 15 μm^2 and 1706 ± 11 μm^2, respectively, Figure 7B). To confirm that K^+ restriction differently impacts muscle structure in WT and GDF15-KO mice, we performed NMR imaging of hindlimbs to precisely measure the size of the muscles. As shown in Figure 7C, the size of the muscles is 2-times smaller in GDF15-KO mice than that of the WT mice after 4 days of K^+ restriction. These two results (laminin labeling and NMR imaging) strongly suggest that GDF15-KO mice lose muscle in response to K^+ restriction whereas WT mice, which have the ability to release K^+ from their muscles, maintain their muscle integrity. Therefore, we, measured markers of muscle degradation and showed that the muscle expression of two genes related to muscle atrophy, TRIM63 and Fxbo32,[31] was strongly upregulated under low-K^+ diet in GDF15-KO mice compared to the WT mice (Figure 7D,E).

3 | DISCUSSION

GDF15 is generally expressed at a low level under normal/healthy conditions, whereas its plasma concentration or urine excretion increase significantly following different stresses that generally involve mitochondrial dysfunction.[32–34] Among its different roles that have been demonstrated (for review, see Ref. 14), its role as an anorectic factor that induces reduction in food intake and weight is of major importance.[35,36] Interestingly, aging and cachexia can also induce GDF15 production,[37] which may trigger a vicious circle leading to decreased appetite further aggravating the state of cachexia. GDF15 plays a role in negative feedback in response to obesity, limiting energy intake and storage (for review, see Ref. 38). In addition to these global

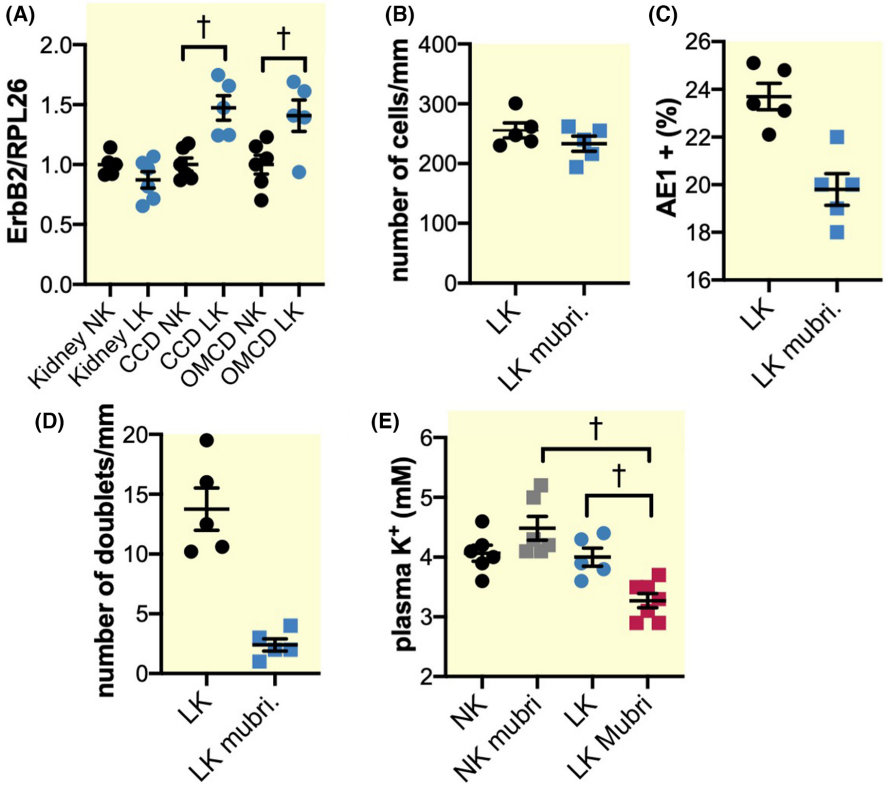

FIGURE 6 ErbB2 receptor mediates the cell proliferation induced by a low-K^+ diet. (A) mRNA expression of ErbB2 in total kidney CCD and OMCD renal segments of mice under normal diet (NK, empty symbols) or K^+-restriction for 4 days (LK, filled symbols). Results are shown as mean ± s.e.m (one series, $n = 5–6$) and analyzed by comparing the effect of the diet on each segment independently of the others by a Mann–Whitney test ($^{\dagger}p < 0.01$; $^{*}p < 0.05$). Number of nucleus (B), percentage of AE1+ cells (C) and the number of AE1+ doublets (D) in WT mice under low-K^+ diet for 4 days (LK) in the absence (blue filled circles) or the presence (green filled squares) of mubritinib treatment. Each symbol represents the mean value of 7–11 reconstructed tubules of the same animal. Results are shown as mean ± s.e.m (one series, $n = 4–5$) and analyzed by a Mann–Whitney test ($^{\dagger}p < 0.01$). (E) Plasma K^+ level in WT mice under control condition (NK, black symbols) and at Day 4 of a low-K^+ diet (LK, blue symbols) in the absence or presence (grey and red symbols) of mubritinib treatment. Results are shown as mean ± s.e.m. (one series, $n = 5–7$) and analyzed by a two-way ANOVA followed by a Sidak's multiple comparison test ($^{\dagger}p < 0.01$; $^{*}p < 0.05$). Plasma K^+ level is not significantly impacted by the treatment but depends on the diet ($p < 0.01$) and the interaction of both ($p < 0.01$).

metabolic effects, GDF15 is also a marker of solid cancer tumor progression and has the potential to be used as a prognostic factor (for review, see Ref. 39). Regarding kidney, GDF15 has been recently identified as a protective factor in acute and chronic kidney disease,[40] promoting tubular cell proliferation and limiting fibrosis.[41]

3.1 | GDF15 regulates renal ion excretion

We recently added to this list of functions the involvement of GDF15 in the control of ionic balances. Indeed, we described that GDF15 expression was strongly increased in kidney collecting ducts in response to acid load[12] and showed that it mediates the proliferation rate of AIC in this condition.[13] The mechanism of this process was recently elucidated; it was shown that GDF15 is produced by principal cells through a vasopressin-dependent pathway and then could activate ErbB2 receptor on AIC either directly or indirectly to trigger cell division.[25] In this study, we showed that GDF15 expression by collecting duct is not specific to metabolic acidosis, but is also induced by K^+ restriction and is systemic, with increased expression in all renal segments and several different gut segments, leading to an overall increase in urinary and circulating levels of GDF15. Acidosis and K^+ restriction are well-known conditions, which lead to increasing numbers of AIC. There is evidence in the literature not only for an increase in the proliferation rate of these cells in both conditions[11,13,25,42] but also for interconversion from one type of cell (principal or BIC) into AIC.[10,43,44] We cannot definitively conclude the involvement of GDF15 in one mechanism or another, but the appearance of AIC doublets under increased level of GDF15 AIC and their decreased frequency in the absence of GDF15 suggest that GDF15 has a role in the proliferation of AIC. In this study, we investigated the consequences of K^+ depletion of extra-renal origin induced by a total lack of K^+ in the diet. This is a

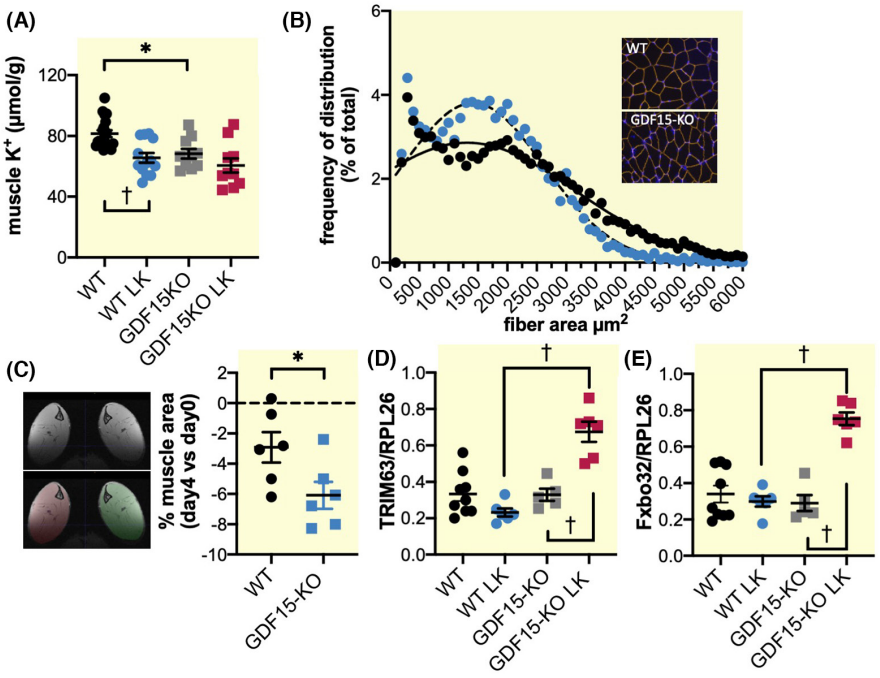

FIGURE 7 Muscle differentially contributes to K^+ balance in WT and GDF15-KO mice. (A) Muscle K^+ content from gastronecmius of WT (blue circles) and GDF15-KO (red squares) mice under normal diet (empty symbols) and LK diet (Day 4, filled symbols). Results are shown as mean ± s.e.m (one series, $n = 5$) and analyzed by one-way ANOVA test and Tukey's post-test (*$p < 0.05$). (B) Distribution of the frequency of muscle fiber area in quadriceps of WT (black circles, plain line) and GDF15-KO (blue circles, dotted line) mice under LK diet for 4 days (bin width 100 µm^2, one series, $n = 3$ mice, 2 slices/mouse, 8197 and 8734 fibers) analyzed in WT and GDF15-KO mice, respectively. Gaussian curves were fitted to the data of WT and GDF15-KO mice, respectively. (C) Example of the NMR images of the hindlimb muscles from a WT mouse under low-K diet. Colored portions correspond to the region of interest (ROI) used for calculation of the muscle area. Measurements were performed in WT (circles) and GDF15-KO (squares) mice in normal K^+ diet and after 4 days of low-K^+ diets. For the same animals, the differences of the muscle surfaces, between the day before diet modification and the Day 4 of the LK diet, were calculated. Results are shown as mean ± s.e.m (one series, $n = 6$) and analyzed by a nonpaired Student t-test (*$p < 0.05$). (D–E) mRNA expression of TRIM63 and Fxbo32 in muscles from WT (circles) and GDF15-KO (squares) mice under normal or LK diet (Day 4). Results are shown as mean ± s.e.m (one series, $n = 6$) and analyzed by two-way ANOVA test and Tukey's post-test ($^\dagger p < 0.01$). For both markers, their expression is significantly impacted by the genotype of the mice ($p < 0.01$), the diet condition ($p < 0.01$) and the interaction of both ($p < 0.01$).

stronger challenge than that faced by people fed a westernized diet. However, this westernized diet accumulates challenges, such as acidosis resulting from consumption of acid-producing foods, which can compound and contribute to an elevation in GDF15. K^+ depletion can also have renal origin,[45] for example, in tubulopathies such as Bartter or Gitelman syndrome or their "pharmacological" equivalent, excess of furosemide or thiazide. In these contexts, we do not know yet whether GDF15 production is stimulated or whether the cell composition of collecting duct is modified. It has to be noted that extra- and intrarenal origin of K^+ depletion and hypokalemia result from different mechanisms, the first being accompanied by a strong decrease of aldosterone whereas the second is mediated by an elevation in aldosterone production. Further investigations, specifically targeting hypokalemia of renal origin, will be required to determine whether GDF15 and collecting remodeling are relevant in this specific situation.

3.2 | A GDF15-ErbB2-HKA2 axis contributing to AIC proliferation

Interestingly, the absence of GDF15 also blunts the stimulation of the H,K-ATPase type 2 expression. This transporter is involved in the process of K^+ retention in different physiological conditions (for review, see Ref. 46). It has also been described as playing a role in cell proliferation/apoptosis balance[47] and is found upregulated in cancer tumors.[48,49] Therefore, this pump could be required to sustain AIC proliferation, a cell type that is almost devoid of Na,K-ATPase,[50,51] to stimulate K^+ uptake and get rid of protons generated by the high metabolic level during division. When GDF15 is not present, the cells would not receive the signal to proliferate. However, in the absence of HKA2, since GDF15 is increased, the cells would receive the signal to start proliferation, but their division would be aborted due to CHOP activation which triggers apoptosis.[52]

The absence of GDF15 impedes the increase of AIC number in response to K^+ restriction, by a mechanism that, as in acidosis,[25] involves ErbB2 receptor. In most of the peripheral tissues such as the kidney, the GDF15 receptor GFRAL is absent,[53] indicating that the peripheral action of this factor must be transduced by another receptor. Whether GDF15 directly binds to ErbB2 receptor remains to be established, however, it is involved in the activation of this receptor in different types of cancer[54–56] where it promotes cell proliferation and pErbB2 was successfully immunoprecipitated with GDF15.[57] The consequences of this inadaptation are a loss of K^+ in the urine and a rapid decrease in the plasma K^+ level, indicating that GDF15-mediated AIC proliferation is of major importance in response to K^+ restriction. Therefore, we established that GDF15 and ErbB2 activation contribute to cell proliferation (Figure 8) and that HKA2 overexpression is required for this process.

3.3 | Extrarenal role of GDF15 in response to K^+ depletion

The finding that induction of GDF15 is not only restricted to a particular renal segment but also to parts of the gut is in agreement with the recent observation that after treatment with metformin, an anti-diabetic drug,[58] the source of GDF15 was the ileum and distal colon.[59] There are also many examples showing that muscle produces GDF15 in different contexts such as exercise[60] or cachexia.[37] In our experiments, after 4 days of dietary K^+ restriction, the expression of GDF15 by muscle was not significantly increased but the tendency we observed suggests that further experiments should be performed to investigate whether the duration of the diet could influence the response of this tissue.

It is proposed that the gut has the ability to sense K^+ content and may release factors that permit the body to rapidly adapt K^+ loading by excreting urine K^+ without any modification of the plasma K^+ level. Elegant works, mainly by J.H. Youn and A.A. McDonough, using the "K^+-clamp" technique (for review, see Ref. 61) and established the concept of feedforward control of K^+ balance. At that time, the proposed factors involved in the feedforward control system were not formally identified and were supposed to "inform" the kidney in a situation of K^+ loading to increase its excretion in the urine. We propose that this system, through GDF15, may also contribute to activating renal K^+ retention mechanisms to prevent a drop in plasma K^+ level in case of low K^+ intake.

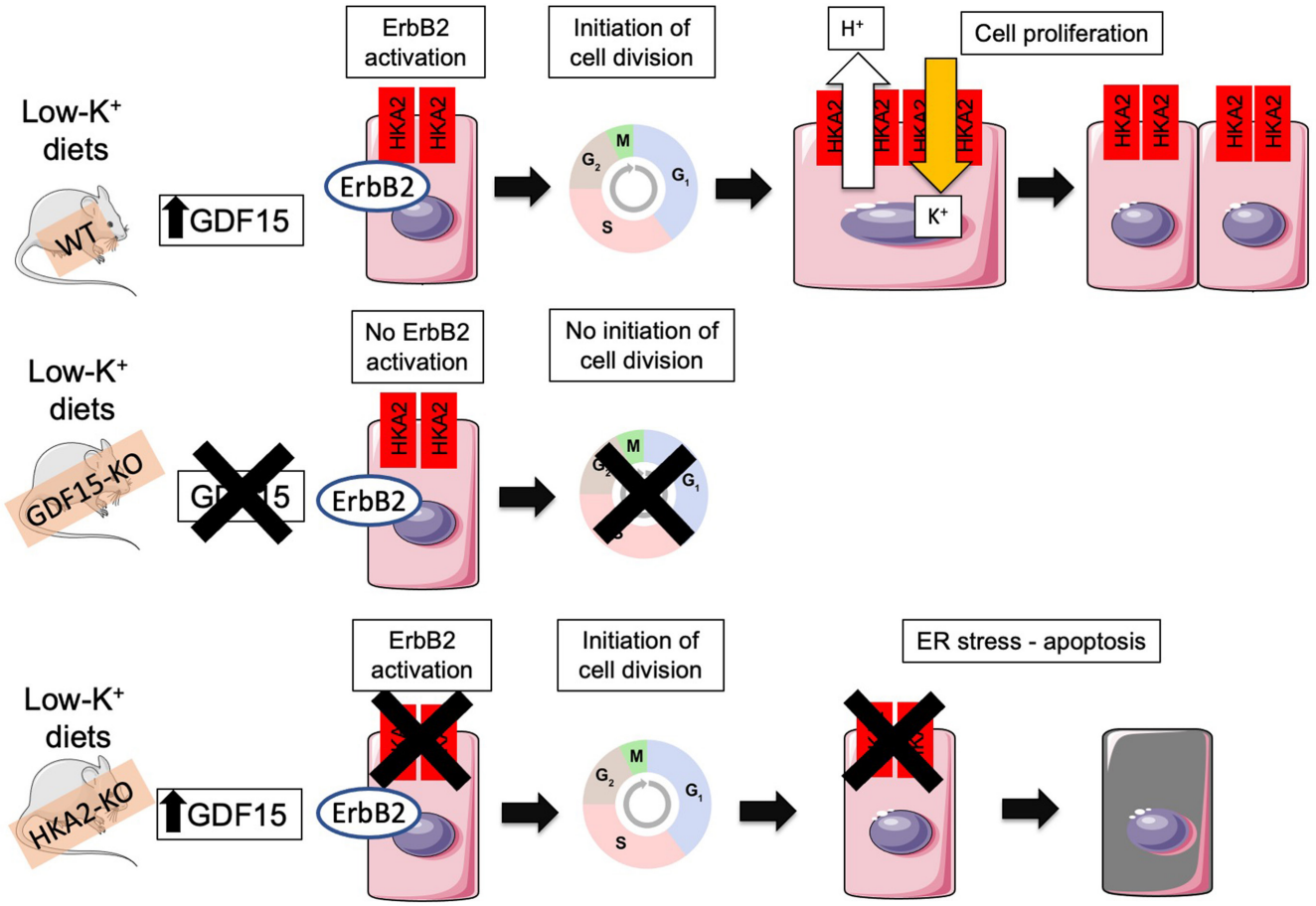

FIGURE 8 Summary scheme of the action of GDF15 and HKA2 in the K^+-restriction-induced AIC proliferation.

Muscle also contributes to maintaining a normal plasma K^+ value when K^+ restriction occurs by limiting the storage of K^+[6,62] through the impairment of the insulin-mediated activation of the Na,K-ATPase.[63] However, GDF15-KO mice have a low muscle K^+ content at baseline and seem unable to reduce it further. Instead, we observed that GDF15-KO mice decreased their muscle volume through GDF15-independent mechanisms. A simple explanation is that a low intracellular K^+ concentration is associated with cell death[64] because it hyperpolarizes the membrane, activates Cl^- secretion and cell shrinkage, and ultimately leads to apoptosis. Therefore, in GDF15-KO mice, since their level of intracellular K^+ is already low, the release of K^+ from muscle cells, as expected in response to K^+ restriction, rapidly leads to muscle cell shrinkage and destruction. In our study, we cannot distinguish between cell shrinkage and cell death to explain the decrease in muscle volume, but both processes are likely involved since we observed the presence of muscle lysis markers. Potassium release via muscle lysis is inefficient to maintain the plasma K^+ value in a normal range in GDF15-KO mice since their kidneys do not retain K^+. Therefore, this is an example where the absence of GDF15 leads to a loss of muscle whereas, in other circumstances, GDF15 is described as a muscle atrophic factor.[15,65]

Altogether, GDF15 appears to be a factor that regulates plasma K^+ level by regulating the renal cell plasticity. Its absence induces a compensatory mechanism that leads to muscle atrophy.

4 | MATERIALS AND METHODS

All material submitted conforms with good publishing practice in physiology.[66]

4.1 | Animals

Experiments were performed on male C57BL/6J wild-type, knock-out mice for the *Gdf15* gene (GDF15-KO) or the *Atp12a* gene[67] (HKA2-KO). The GDF15-KO mice were first provided by Dr. Se-Jin Lee (John Hopkins University, Baltimore, MD) and backcrossed then with C57BL/6J.[13] The absence of GDF15 expression in the GDF15-KO mice was confirmed by ELISA measurement in plasma. Both colonies are regularly (every 5–10 generations) backcrossed with wild-type C57BL/6J male mice from the Janvier Labs to avoid genetic deviation. The animals were kept at CEF (Centre d'Explorations Fonctionnelles of the Cordeliers Research Center, Agreement no. A75-06-12).

4.2 | Metabolic analysis

To record physiological parameters, mice were placed in metabolic cages (Techniplast, France) for 2 days of adaptation and were fed a standard laboratory diet (0.3% Na^+ and 0.6% K^+; UPAE, INRA, Jouy-en-Josas, France) or a low-K^+ diet (0.28% Na^+ and 0.01% K^+; UPAE, INRA, Jouy-en-Jossas, France). Time in metabolic cages did not exceed 5 consecutive days. After measuring urine excretion, the mice are returned to normal cages with their attributed diet for a period of 2 days. Mubritinib (Euromedex, Souffelweyersheim, France) treatment was performed by gavage twice daily (8 mg/kg/day) for 4 days along with a normal or a low-K^+ diet.

Urinary creatinine concentrations were determined using an automatic analyzer (Konelab 20i; Thermo). Urinary K^+ concentration was determined by flame photometry (M420, Sherwood Scientific, France). Plasma K^+ was measured by retro-orbital puncture on the anesthetized animal (a mix of xylazine, 10 mg/kg and ketamine 100 mg/kg) with an Epoc pH/blood-gas analyzer (Siemens Healthineers). Plasma and urine GDF15 were measured by ELISA test (MG150 and DGD150, for rodent and human GDF15, respectively, R&D Systems) and tissue GDF15 was measured using an ELISA test (Elabscience).

4.3 | Quantitative PCR

After collection, mRNA of kidney, muscle and part of the gut were extracted by the TRI reagent (Invitrogen) following the manufacturer's instructions. Isolation of 40–60 renal segments was performed according to localization in the kidney (cortex vs. medulla) and well-defined morphologic characteristics under binocular loupes after kidney treatment with Liberase (Sigma-Aldrich) as described in Ref. 25 RNA extraction from these segments was performed using RNeasy micro kit (Qiagen). mRNA was then retro-transcribed into cDNA (Roche Diagnostics) according to the manufacturer's instructions and real-time PCRs were performed on a LightCycler (Roche Diagnostics). No signal was detected in samples that did not undergo reverse transcription or in blank runs without cDNA. In each run, a standard curve was obtained using serial dilution of stock cDNA. The expression of the housekeeping genes such as *Ppia or Rpl26* is used to normalize the results.

4.4 | Western blot analysis

Whole kidneys were homogenized in a lysis buffer (250 mM sucrose, 100 mM Tris-Hepes, pH 7.4) and

protease inhibitor cocktail (Complete, Roche Diagnostics). After removal of aggregates and nuclear-associated membrane by low-speed centrifugations, the supernatant was recovered into the lysis buffer, and its protein content was measured with the BCA method (Thermo Scientific Pierce). Fifteen micrograms of protein were separated on a 10% polyacrylamide gel, after migration at 125 V in migration buffer (25 mM Tris, 0.2 M Glycine, 0.1% SDS). The gels were then electrotransferred onto a nitrocellulose membrane in transfer buffer (25 mM Tris, 2 M Glycine, 0.02% SDS, 20% Ethanol for 1 hour 30 min at 25 V). The quality of the transfer was checked by staining with ponceau red. After rinsing with 0.05% PBS-Tween, the nonspecific antigenic sites were blocked by incubating the membranes in a solution containing 5% skim milk dissolved in 0.05% PBS-Tween for 1 h, with stirring, at room temperature. After saturation, the membranes were incubated (overnight at 4°C) with the primary mouse anti-CHOP antibody (1:1000, Cell Signaling Technology). After washing in 0.05% PBS-Tween, the membranes are incubated with the secondary antibody (anti-mouse 1:10 000, Cell Signaling Technology) coupled to HorseRaddish Peroxidase (HRP) diluted in 5% milk and PBS-Tween 0.05% for 1 h with stirring at room temperature. After washing, the presence of a marking was revealed by the ECL method in accordance with the supplier's instructions (Thermo scientific).

4.5 | Immunolabeling on isolated OMCD for cell counting and TUNEL assay

Fifteen to twenty short OMCD segments were isolated from Liberase-treated kidney and transferred onto Superfrost Plus glass slides and treated as described recently in Ref. 25. AIC were identified as AE1+ cells after labeling with an anti-AE1 antibody (1/500, gift from C.A. Wagner). For cell and doublet counting, a 3D reconstruction from all stacks (ImageJ) was performed from images of AE1-labeled OMCDs acquired by confocal microscopy.[25] Labeling of cells in apoptosis was done with the Dead-End™ Fluorometric TUNEL System Kit (PROMEGA) as indicated in the protocol provided.

4.6 | Immunolabeling for laminin on muscle tissues

Quadriceps were collected and fixed in 4% paraformaldehyde (PFA) solution for 1 h, rinsed in PBS for 30 min, and immediately frozen in optimum cutting temperature medium (OCT). Four µm-thick sections were cut with a cryostat (Leica CM305S). Before labeling with a rabbit anti-laminine (1/400 Abcam, ab11575) and a secondary anti-rabbit antibody (Alexa Fluor 555, Abcam), the slices underwent a retrieval procedure (Tris-EDTA pH 9, 10 min, 95°C). The labeled slices were then observed using an Axio Scan Z1 (Zeiss) microscope allowing acquisition of whole slice images. The muscle fiber areas were determined using the QuPath software,[68] and the frequencies of distribution were assessed using GraphPad Prism software.

4.7 | NMR imaging of mouse hindlimbs

NMR experiments were performed on WT and GDF15-KO mice ($n = 6$) at baseline and 4 days after Low-K^+ diet. NMR data were acquired using a 7T Bruker BioSpec system interfaced with an Advance III spectrometer (Bruker BioSpin MRI GmbH). Mice were scanned under isoflurane anesthesia (1%–2%, 1 L/min O_2) on a water-heating pad. Respiratory frequency was maintained between 80 and 100 motions/min. The NMR setup used was a ^{1}H transceiver surface Cryoprobe placed next to the anterior compartment of the two hindlimbs. Muscle atrophy was evaluated from the maximum cross-sectional area of the legs (CSAmax) measured on one slice from an axial high-resolution ($50 \times 50 \times 200\ \mu m^3$) gradient-echo images (12 slices, slice gap = 0.5 mm, TE = 3.66 ms, TR = 166.26 ms, FA = 25°, NA = 12, acquisition time = 8 min 18 s). Contours of the legs were drawn using ITK-SNAP 3.8.0 (Free Software Foundation, Inc) software.

4.8 | Data and statistical analysis

Results are expressed as mean ± s.e.m. The numbers of mice used in these experiments are indicated in the legends (n). The normality of the result distribution was tested using the Shapiro–Wilk analysis. Nonparametric (One-way or two-way ANOVA tests) or parametric (Student t-test) tests were used to determine statistical significance (see the legends), differences with $p < 0.05$ were considered significant. Original data arising from this research are available directly from G.C. upon reasonable request.

4.9 | Study approvals

All animal experimentations were conducted in accordance with the institutional guidelines and the recommendations for the care and use of laboratory animals put forward by the Directive 2010/63/EU revising Directive

86/609/EEC on the protection of animals used for scientific purposes (project has been approved by a user establishment's ethics committee and the Project Authorization: number 21927).

AUTHOR CONTRIBUTIONS

Samia Lasaad: Conceptualization; investigation; formal analysis; writing – original draft; methodology. **Christine Walter:** Conceptualization; methodology; investigation. **Chloé Rafael:** Conceptualization; methodology; investigation. **Luciana Morla:** Conceptualization; methodology; investigation. **Alain Doucet:** Validation; formal analysis; supervision. **Nicolas Picard:** Validation; supervision; formal analysis. **Anne Blanchard:** Validation; formal analysis; supervision. **Yves Fromes:** Conceptualization; investigation; formal analysis. **Béatrice Matot:** Conceptualization; investigation; formal analysis. **Gilles Crambert:** Conceptualization; validation; supervision; writing – original draft; writing – review and editing. **Lydie Cheval:** Conceptualization; investigation; validation; supervision; writing – original draft.

ACKNOWLEDGMENTS

Physiological studies have been performed with the help of Gaëlle Brideau and Nadia Frachon from the "plateforme d'exploration fonctionnelle du petit animal" of the team "Physiologie Rénale and Tubulopathies" at the Centre de Recherche des Cordeliers. We are grateful for the technical assistance of the Centre d'Exploration Fonctionelle crews in the management of our colonies of mice. We warmly thank Francisco Carattino from Icahn School of Medicine at Mount Sinai (New York City, New York, United States) for his careful reading of the manuscript. This study was supported by the Agence National de la Recherche (ANR) project ANR-21-CE14-0040-01. S.L. was supported by the Ministère de l'Enseignement Supérieur, de la Recherche et de l'Innovation.

CONFLICT OF INTEREST STATEMENT

The authors have declared that no conflict of interest exists.

DATA AVAILABILITY STATEMENT

Original data arising from this research are available directly from G.C. upon reasonable request.

ORCID

Nicolas Picard https://orcid.org/0000-0002-1695-3389
Gilles Crambert https://orcid.org/0000-0001-7065-9124

REFERENCES

1. Sebastian A, Frassetto LA, Sellmeyer DE, Merriam RL, Morris RC Jr. Estimation of the net acid load of the diet of ancestral preagricultural Homo sapiens and their hominid ancestors. *Am J Clin Nutr*. 2002;76:1308-1316. doi:10.1093/ajcn/76.6.1308
2. Meneton P, Loffing J, Warnock DG. Sodium and potassium handling by the aldosterone-sensitive distal nephron: the pivotal role of the distal and connecting tubule. *Am J Physiol Renal Physiol*. 2004;287:F593-F601.
3. Blanchard A, Brailly Tabard S, Lamaziere A, et al. Adrenal adaptation in potassium-depleted men: role of progesterone? *Nephrol Dial Transplant*. 2020;35:1901-1908. doi:10.1093/ndt/gfz135
4. Mente A, O'Donnell MJ, Rangarajan S, et al. Association of urinary sodium and potassium excretion with blood pressure. *N Engl J Med*. 2014;371:601-611. doi:10.1056/NEJMoa1311989
5. O'Donnell M, Mente A, Rangarajan S, et al. Urinary sodium and potassium excretion, mortality, and cardiovascular events. *N Engl J Med*. 2014;371:612-623. doi:10.1056/NEJMoa1311889
6. McDonough AA, Thompson CB, Youn JH. Skeletal muscle regulates extracellular potassium. *Am J Physiol Renal Physiol*. 2002;282:F967-F974. doi:10.1152/ajprenal.00360.2001
7. Choi CS, Thompson CB, Leong PK, McDonough AA, Youn JH. Short-term K(+) deprivation provokes insulin resistance of cellular K(+) uptake revealed with the K(+) clamp. *Am J Physiol Renal Physiol*. 2001;280:F95-F102.
8. Wang W. Regulation of renal K transport by dietary K intake. *Annu Rev Physiol*. 2004;66:547-569.
9. Elabida B, Edwards A, Salhi A, et al. Chronic potassium depletion increases adrenal progesterone production that is necessary for efficient renal retention of potassium. *Kidney Int*. 2011;80:256-262. doi:10.1038/ki.2011.15
10. Park EY, Kim WY, Kim YM, et al. Proposed mechanism in the change of cellular composition in the outer medullary collecting duct during potassium homeostasis. *Histol Histopathol*. 2012;27:1559-1577. doi:10.14670/HH-27.1559
11. Cheval L, Duong van Huyen JP, Bruneval P, Verbavatz JM, Elalouf JM, Doucet A. Plasticity of mouse renal collecting duct in response to potassium depletion. *Physiol Genomics*. 2004;19:61-73.
12. Cheval L, Morla L, Elalouf JM, Doucet A. Kidney collecting duct acid–base "regulon". *Physiol Genomics*. 2006;27:271-281.
13. Duong Van Huyen JP, Cheval L, Bloch-Faure M, et al. GDF15 triggers homeostatic proliferation of acid-secreting collecting duct cells. *J Am Soc Nephrol*. 2008;19:1965-1974. doi:10.1681/ASN.2007070781
14. Assadi A, Zahabi A, Hart RA. GDF15, an update of the physiological and pathological roles it plays: a review. *Pflugers Arch*. 2020;472:1535-1546. doi:10.1007/s00424-020-02459-1
15. Mulderrig L, Garaycoechea JI, Tuong ZK, et al. Aldehyde-driven transcriptional stress triggers an anorexic DNA damage response. *Nature*. 2021;600:158-163. doi:10.1038/s41586-021-04133-7
16. Cimino I, Kim H, Tung YCL, et al. Activation of the hypothalamic-pituitary-adrenal axis by exogenous and endogenous GDF15. *Proc Natl Acad Sci U S A*. 2021;118:e2106868118. doi:10.1073/pnas.2106868118
17. Poulsen NS, Madsen KL, Hornsyld TM, et al. Growth and differentiation factor 15 as a biomarker for mitochondrial myopathy. *Mitochondrion*. 2020;50:35-41. doi:10.1016/j.mito.2019.10.005
18. Fujita Y, Ito M, Kojima T, Yatsuga S, Koga Y, Tanaka M. GDF15 is a novel biomarker to evaluate efficacy of pyruvate therapy

for mitochondrial diseases. *Mitochondrion*. 2015;20:34-42. doi:10.1016/j.mito.2014.10.006
19. Fujita Y, Taniguchi Y, Shinkai S, Tanaka M, Ito M. Secreted growth differentiation factor 15 as a potential biomarker for mitochondrial dysfunctions in aging and age-related disorders. *Geriatr Gerontol Int*. 2016;16(Suppl 1):17-29. doi:10.1111/ggi.12724
20. Xiong Y, Walker K, Min X, et al. Long-acting MIC-1/GDF15 molecules to treat obesity: evidence from mice to monkeys. *Sci Transl Med*. 2017;9:eaan8732. doi:10.1126/scitranslmed.aan8732
21. Tsai VW, Zhang HP, Manandhar R, et al. Treatment with the TGF-b superfamily cytokine MIC-1/GDF15 reduces the adiposity and corrects the metabolic dysfunction of mice with diet-induced obesity. *Int J Obes (Lond)*. 2018;42:561-571. doi:10.1038/ijo.2017.258
22. Ost M, Igual Gil C, Coleman V, et al. Muscle-derived GDF15 drives diurnal anorexia and systemic metabolic remodeling during mitochondrial stress. *EMBO Rep*. 2020;21:e48804. doi:10.15252/embr.201948804
23. Tsai VW, Macia L, Johnen H, et al. TGF-b superfamily cytokine MIC-1/GDF15 is a physiological appetite and body weight regulator. *PLoS ONE*. 2013;8:e55174. doi:10.1371/journal.pone.0055174
24. Tanaka T, Biancotto A, Moaddel R, et al. Plasma proteomic signature of age in healthy humans. *Aging Cell*. 2018;17:e12799. doi:10.1111/acel.12799
25. Cheval L, Viollet B, Klein C, et al. Acidosis-induced activation of distal nephron principal cells triggers Gdf15 secretion and adaptive proliferation of intercalated cells. *Acta Physiol (Oxf)*. 2021;232:e13661. doi:10.1111/apha.13661
26. Marakhova II, Vinogradova TA, Yefimova EV. Early and delayed changes in potassium transport during the initiation of cell proliferation in CHO culture. *Gen Physiol Biophys*. 1989;8:273-282.
27. Marakhova I, Yurinskaya V, Aksenov N, Zenin V, Shatrova A, Vereninov A. Intracellular K(+) and water content in human blood lymphocytes during transition from quiescence to proliferation. *Sci Rep*. 2019;9:16253. doi:10.1038/s41598-019-52571-1
28. Putney LK, Barber DL. Na–H exchange-dependent increase in intracellular pH times G2/M entry and transition. *J Biol Chem*. 2003;278:44645-44649. doi:10.1074/jbc.M308099200
29. Lang F, Hoffmann EK. Role of ion transport in control of apoptotic cell death. *Compr Physiol*. 2012;2:2037-2061. doi:10.1002/cphy.c110046
30. Breit SN, Brown DA, Tsai VW. The GDF15-GFRAL pathway in health and metabolic disease: friend or foe? *Annu Rev Physiol*. 2021;83:127-151. doi:10.1146/annurev-physiol-022020-045449
31. Bodine SC, Latres E, Baumhueter S, et al. Identification of ubiquitin ligases required for skeletal muscle atrophy. *Science*. 2001;294:1704-1708. doi:10.1126/science.1065874
32. Kalko SG, Paco S, Jou C, et al. Transcriptomic profiling of TK2 deficient human skeletal muscle suggests a role for the p53 signalling pathway and identifies growth and differentiation factor-15 as a potential novel biomarker for mitochondrial myopathies. *BMC Genomics*. 2014;15:91. doi:10.1186/1471-2164-15-91
33. Montero R, Yubero D, Villarroya J, et al. GDF-15 is elevated in children with mitochondrial diseases and is induced by mitochondrial dysfunction. *PLoS ONE*. 2016;11:e0148709. doi:10.1371/journal.pone.0148709
34. Yatsuga S, Fujita Y, Ishii A, et al. Growth differentiation factor 15 as a useful biomarker for mitochondrial disorders. *Ann Neurol*. 2015;78:814-823. doi:10.1002/ana.24506
35. Chrysovergis K, Wang X, Kosak J, et al. NAG-1/GDF-15 prevents obesity by increasing thermogenesis, lipolysis and oxidative metabolism. *Int J Obes (Lond)*. 2014;38:1555-1564. doi:10.1038/ijo.2014.27
36. Tran T, Yang J, Gardner J, Xiong Y. GDF15 deficiency promotes high fat diet-induced obesity in mice. *PLoS ONE*. 2018;13:e0201584. doi:10.1371/journal.pone.0201584
37. Jones JE, Cadena SM, Gong C, et al. Supraphysiologic administration of GDF11 induces cachexia in part by upregulating GDF15. *Cell Rep*. 2018;22:3375. doi:10.1016/j.celrep.2018.03.024
38. Hale C, Veniant MM. Growth differentiation factor 15 as a potential therapeutic for treating obesity. *Mol Metab*. 2021;46:101117. doi:10.1016/j.molmet.2020.101117
39. Wischhusen J, Melero I, Fridman WH. Growth/differentiation factor-15 (GDF-15): from biomarker to novel targetable immune checkpoint. *Front Immunol*. 2020;11:951. doi:10.3389/fimmu.2020.00951
40. Valino-Rivas L, Cuarental L, Ceballos MI, et al. Growth differentiation factor-15 preserves Klotho expression in acute kidney injury and kidney fibrosis. *Kidney Int*. 2022;101:1200-1215. doi:10.1016/j.kint.2022.02.028
41. Kim YI, Shin HW, Chun YS, Park JW. CST3 and GDF15 ameliorate renal fibrosis by inhibiting fibroblast growth and activation. *Biochem Biophys Res Commun*. 2018;500:288-295. doi:10.1016/j.bbrc.2018.04.061
42. Kimura T, Nishino T, Maruyama N, et al. Expression of Bcl-2 and Bax in hypokalemic nephropathy in rats. *Pathobiology*. 2001;69:237-248. doi:10.1159/000064334
43. Gao X, Eladari D, Leviel F, et al. Deletion of hensin/DMBT1 blocks conversion of β- to α-intercalated cells and induces distal renal tubular acidosis. *Proc Natl Acad Sci U S A*. 2010;107:21872-21877. doi:10.1073/pnas.1010364107
44. Iervolino A, Prosperi F, de la Motte LR, et al. Potassium depletion induces cellular conversion in the outer medullary collecting duct altering notch signaling pathway. *Sci Rep*. 2020;10:5708. doi:10.1038/s41598-020-61882-7
45. Tabibzadeh N, Crambert G. Mechanistic insights into the primary and secondary alterations of renal ion and water transport in the distal nephron. *J Intern Med*. 2023;293:4-22. doi:10.1111/joim.13552
46. Crambert G. H-K-ATPase type 2: relevance for renal physiology and beyond. *Am J Physiol Renal Physiol*. 2014;306:F693-F700. doi:10.1152/ajprenal.00605.2013
47. Jakab M, Hofer S, Ravasio A, et al. The putative role of the non-gastric H(+)/K(+)-ATPase ATP12A (ATP1AL1) as anti-apoptotic ion transporter: effect of the H(+)/K(+) ATPase inhibitor SCH28080 on butyrate-stimulated myelomonocytic HL-60 cells. *Cell Physiol Biochem*. 2014;34:1507-1526. doi:10.1159/000366355
48. Kong SC, Gianuzzo A, Novak I, Pedersen SF. Acid–base transport in pancreatic cancer: molecular mechanisms and clinical potential. *Biochem Cell Biol = Biochimie et Biologie Cellulaire*. 2014;92:449-459. doi:10.1139/bcb-2014-0078
49. Streif D, Iglseder E, Hauser-Kronberger C, Fink KG, Jakab M, Ritter M. Expression of the non-gastric H+/K+ ATPase ATP12A in normal and pathological human prostate tissue. *Cell Physiol Biochem*. 2011;28:1287-1294. doi:10.1159/000335860
50. Kashgarian M, Biemesderfer D, Caplan M, Forbush B 3rd. Monoclonal antibody to Na,K-ATPase: immunocytochemical localization along nephron segments. *Kidney Int*. 1985;28:899-913. doi:10.1038/ki.1985.216

51. Holthofer H, Schulte BA, Pasternack G, Siegel GJ, Spicer SS. Three distinct cell populations in rat kidney collecting duct. *Am J Physiol*. 1987;253:C323-C328. doi:10.1152/ajpcell.1987.253.2.C323
52. McCullough KD, Martindale JL, Klotz LO, Aw TY, Holbrook NJ. Gadd153 sensitizes cells to endoplasmic reticulum stress by down-regulating Bcl2 and perturbing the cellular redox state. *Mol Cell Biol*. 2001;21:1249-1259. doi:10.1128/MCB.21.4.1249-1259.2001
53. Mullican SE, Lin-Schmidt X, Chin CN, et al. GFRAL is the receptor for GDF15 and the ligand promotes weight loss in mice and nonhuman primates. *Nat Med*. 2017;23:1150-1157. doi:10.1038/nm.4392
54. Lv C, Li S, Zhao J, Yang P, Yang C. M1 macrophages enhance survival and invasion of oral squamous cell carcinoma by inducing GDF15-mediated ErbB2 phosphorylation. *ACS Omega*. 2022;7:11405-11414. doi:10.1021/acsomega.2c00571
55. Joshi JP, Brown NE, Griner SE, Nahta R. Growth differentiation factor 15 (GDF15)-mediated HER2 phosphorylation reduces trastuzumab sensitivity of HER2-overexpressing breast cancer cells. *Biochem Pharmacol*. 2011;82:1090-1099. doi:10.1016/j.bcp.2011.07.082
56. Zhao TC, Zhou ZH, Ju WT, et al. Mechanism of sensitivity to cisplatin, docetaxel, and 5-fluorouracil chemoagents and potential erbB2 alternatives in oral cancer with growth differentiation factor 15 overexpression. *Cancer Sci*. 2022;113:478-488. doi:10.1111/cas.15218
57. Li S, Ma YM, Zheng PS, Zhang P. GDF15 promotes the proliferation of cervical cancer cells by phosphorylating AKT1 and Erk1/2 through the receptor ErbB2. *J Exp Clin Cancer Res*. 2018;37:80. doi:10.1186/s13046-018-0744-0
58. Day EA, Ford RJ, Smith BK, et al. Metformin-induced increases in GDF15 are important for suppressing appetite and promoting weight loss. *Nat Metab*. 2019;1:1202-1208. doi:10.1038/s42255-019-0146-4
59. Coll AP, Chen M, Taskar P, et al. GDF15 mediates the effects of metformin on body weight and energy balance. *Nature*. 2020;578:444-448. doi:10.1038/s41586-019-1911-y
60. Laurens C, Parmar A, Murphy E, et al. Growth and differentiation factor 15 is secreted by skeletal muscle during exercise and promotes lipolysis in humans. *JCI Insight*. 2020;5:e131870. doi:10.1172/jci.insight.131870
61. Youn JH. Gut sensing of potassium intake and its role in potassium homeostasis. *Semin Nephrol*. 2013;33:248-256. doi:10.1016/j.semnephrol.2013.04.005
62. Choi CS, Lee FN, McDonough AA, Youn JH. Independent regulation of in vivo insulin action on glucose versus K(+) uptake by dietary fat and K(+) content. *Diabetes*. 2002;51:915-920. doi:10.2337/diabetes.51.4.915
63. Thompson CB, McDonough AA. Skeletal muscle Na,K-ATPase alpha and beta subunit protein levels respond to hypokalemic challenge with isoform and muscle type specificity. *J Biol Chem*. 1996;271:32653-32658.
64. Yu SP. Regulation and critical role of potassium homeostasis in apoptosis. *Prog Neurobiol*. 2003;70:363-386. doi:10.1016/s0301-0082(03)00090-x
65. Solagna F, Tezze C, Lindenmeyer MT, et al. Pro-cachectic factors link experimental and human chronic kidney disease to skeletal muscle wasting programs. *J Clin Invest*. 2021;131:e135821. doi:10.1172/JCI135821
66. Jensen BL, Persson PB. Good publication practice in physiology 2021. *Acta Physiol (Oxf)*. 2022;234:e13741. doi:10.1111/apha.13741
67. Meneton P, Schultheis PJ, Greeb J, et al. Increased sensitivity to K+ deprivation in colonic H,K-ATPase-deficient mice. *J Clin Invest*. 1998;101:536-542.
68. Bankhead P, Loughrey MB, Fernández JA, et al. QuPath: open source software for digital pathology image analysis. *Sci Rep*. 2017;7:16878. doi:10.1038/s41598-017-17204-5

How to cite this article: Lasaad S, Walter C, Rafael C, et al. GDF15 mediates renal cell plasticity in response to potassium depletion in mice. *Acta Physiol*. 2023;00:1-15. doi:10.1111/apha.14046